



Article

Simulated Photoabsorption Spectra for Singly and Multiply Charged Ions

Stephan Fritzsche 1,2,3,* , Aloka Kumar Sahoo 1,2 , Lalita Sharma 4 and Stefan Schippers 5,6

- ¹ Helmholtz-Institut Jena, Fröbelstieg 3, 07743 Jena, Germany; a.k.sahoo@hi-jena.gsi.de
- ² GSI Helmholtzzentrum für Schwerionenforschung, 64291 Darmstadt, Germany
- Theoretisch-Physikalisches Institut, Friedrich-Schiller-Universität Jena, 07743 Jena, Germany
- Department of Physics, Indian Institute of Technology Roorkee, Roorkee 247667, India; lalita.sharma@ph.iitr.ac.in
- I. Physikalisches Institut, Justus-Liebig-Universität Giessen, 35392 Giessen, Germany; stefan.schippers@uni-giessen.de
- Helmholtz Research Academy Hesse for FAIR (HFHF), GSI Helmholtzzentrum für Schwerionenforschung, Campus Giessen, 35392 Giessen, Germany
- * Correspondence: s.fritzsche@gsi.de

Abstract

Simulated (or measured) photoabsorption spectra often provide the first indication of how matter interacts with light when irradiated by some radiation source. In addition to the direct, often slowly varying photoabsorption cross-section as a function of the incident photon frequency, such spectra typically exhibit numerous resonances and edges arising from the interaction of the radiation field with the subvalence or even inner-shell electrons. Broadly speaking, these resonances reflect photoexcitation, with its subsequent fluorescence, or the autoionization of bound electrons. Here, a (relativistic) cascade model is developed for estimating the photoabsorption of (many) atoms and multiply charged ions with a complex shell structure across the periodic table. This model helps distinguish between level- and shell-resolved, as well as total photoabsorption, cross-sections, starting from admixtures of selected initial-level populations. Examples are shown for the photo absorption of C^+ ions near the 1s-2p excitation threshold and for Xe^{2+} ions in the photon energy range from 10 to 200 eV. While the accuracy and resolution of the predicted photoabsortion spectra remain limited due to the additive treatment of resonances and because of missing electronic correlations in the representation of the levels involved, the present implementation is suitable for ions with quite different open-shell structures and may support smart surveys of resonances along different isoelectronic sequences.

Keywords: atom; atomic cascade; atomic structure; Jena Atomic Calculator; photoabsorption cross-section; photoexcitation; photoionization; photoresonance; relativistic; shell-resolved and total cross-sections



Academic Editor: Eugene T. Kennedy

Received: 22 July 2025 Revised: 15 August 2025 Accepted: 21 August 2025 Published: 3 September 2025

Citation: Fritzsche, S.; Sahoo, A.K.; Sharma, L.; Schippers, S. Simulated Photoabsorption Spectra for Singly and Multiply Charged Ions. *Atoms* 2025, 13, 77. https://doi.org/ 10.3390/atoms13090077

Copyright: © 2025 by the authors. Licensee MDPI, Basel, Switzerland. This article is an open access article distributed under the terms and conditions of the Creative Commons Attribution (CC BY) license (https://creativecommons.org/licenses/by/4.0/).

1. Introduction

Photoexcitation and ionization are ubiquitous in nature if matter interacts with radiation. The combined effect of these two processes not only characterizes the loss of radiation from a given light source [1,2] but also determines the evolution of chemical reactions [3], the formation of plasma in different environments [4,5], the opacities of stellar atmospheres [6,7], and the modification and regeneration of biological tissues [8], among other impacts. Simulated (or measured) photoabsorption spectra, therefore, often provide

Atoms 2025, 13, 77 2 of 16

a first hint about how ions, atoms, and molecules interact with radiation and which subsequent emission or decay processes actually occur within a given environment. Moreover, since many astrophysical plasmas are both dilute and far from thermodynamic equilibrium, a total photoabsorption cross-section of ions is also essential for modeling the ionization and thermal balances of various astrophysical objects [9,10].

Several elaborate and advanced theoretical methods have been developed in recent decades in order to compute the photoabsorption of light by different materials [11,12]. They have shown that electronic structure theory is indeed effective and powerful, being able to describe the interaction of atoms and ions with the radiation field and that the correlated motion of electrons (beyond the Hartree–Fock level) may play a crucial role in selected situations. Often, however, these methods deal either with small domains of photon energies, or even single resonances [13,14], or they only consider the role of relativistic effects [15] and higher multipoles [16]. All these theoretical studies are typically based on quite a detailed treatment of inter-electronic correlations. In this work, in contrast, we aim to implement a basic cascade model to estimate the photoabsorption cross-sections as a function of energy over a rather wide range of photon frequencies by additively including contributions from different shells. This model is based on JAC, the Jena Atomic Calculator [17], and can be readily applied to distinguish between the non-resonant and resonant parts of the cross-sections. Like for other cascade schemes of JAC [18], the present extension of the code is quite easy to use and provides efficient control of various approximations, shell structures, or admixtures of ions at different initial levels. It can also be applied to compute the photoabsorption cross-sections of ions in initially metastable states, which may occur in astrophysics.

This work is structured as follows. In the next section, we briefly recall the photoabsorption cross-section in terms of the many-electron amplitudes that connect the selected initial levels of the atoms and ions with different final levels due to (i) the direct photoionization of electrons and/or (ii) their resonant excitation with subsequent fluorescence or autoionization. No other photon-matter-scattering process is known to be similarly relevant to the 10–10,000 eV photon energy region of present interest. In Section 3, we then explain how the photoabsorption cross-sections (spectra) can be tabulated (and displayed) for ions with a given shell structure by dealing independently with the photoexcited and/or ionized configurations. As an example, we analyze the photoabsorption cross-sections of carbon ions near the 1s-2p ionization threshold. We also discuss the photoabsorption of Xe^{2+} ions in the photon energy range from 10 and 200 eV, which is relevant for ion thrusters and propulsion systems. Both examples demonstrate how readily JAC can be utilized for modeling photon absorption processes over a wide range of photon energies. Finally, a short summary and conclusions are presented in Section 4.

2. Theory and Computations

2.1. Energy-Dependent Photoabsorption Cross-Sections

Photoabsorption generally comprises all (quantum) processes of matter that annihilate radiation from a light source and, subsequently, lead to the emission of light and particles at various energies, including exotic processes, such as photoluminiscence, the scattering of light, or even the creation or annihilation of (electron–positron) pairs. For neutral atoms or multiply charged ions, as well as for moderate photon energies, however, the photoabsorption can be considered synonymous with the sum of *direct* photoionization and the (*resonant*) excitation of bound electrons due to their coupling to the radiation field. This is summarized in Figure 1. In this approximation, the photoabsorption cross-section of ions at the initial level *i* is usually expressed by the incoherent summation of the (non-resonant)

Atoms 2025, 13, 77 3 of 16

partial photoionization cross-sections of bound electrons, as well as the photoexcitation of the ion, with subsequent fluorescence and/or autoionization, as follows:

$$\sigma^{\text{(absorption)}}\left(\hbar\omega;i\right) \ \approx \ \sum_{f} \sigma^{\text{(ionization)}}\left(\hbar\omega;i\to f\right) \ + \ \sum_{e,f'} \sigma^{\text{(excitation)}}\left(\hbar\omega;i\to e\right) b(e\to f'), \tag{1}$$

where $\sigma^{\text{(ionization)}}(\hbar\omega; i \to f)$ denotes the direct photoionization cross-section into any of the allowed final levels f of the ion and $\sigma^{\text{(excitation)}}(\hbar\omega; i \to e)$ denotes the photoexcitation cross-section into a well-defined (many-electron) resonant level e as it may appear in the interval $[\hbar\omega_{\min}, \hbar\omega_{\max}]$ of given photon energies. Moreover, $b(e \to f')$ refers to the branching fraction (probability) that the formation of the resonance levels e eventually results in the population of some final level f', which is often similar as in the direct photoionization. For a fixed photon energy, moreover, different final levels $\{f\}$ may result also in the emission of electrons with quite different kinetic energies. Typically, in addition, the atoms and ions can be found initially in one of several levels $\{i\}$ with a—more or less—known level composition. For a given photon energy range, the sets of intermediate $\{e\}$ and final levels $\{f\}$ can then be selected automatically by taking the electron-photon interaction into account. While the selection of levels $\{i\}$ and $\{f\}$ is usually determined by the preparation, resolution and goals that are made for some measurement, the set $\{e\}$ generally reflects the details of the electron–electron and electron–photon interaction in matter. All these interactions eventually depend also on the nuclear charge, photon frequency and intensity, the coupling of shells or, just in brief, the detailed electronic structure of the irradiated atoms.

Even from this simplified viewpoint of photoabsorption, the three sets of bound-state levels $\{i\}$, $\{e\}$ and $\{f\}$ make the calculation of simulated absorption spectra quite demanding if requested for a wide domain of photon energies. In atomic structure theory, each level $\alpha \mathbb{J} \equiv \alpha J^P$ is hereby characterized by the total angular momentum J and parity P as well as all further quantum numbers α that are needed for a unique specification of the atomic fine-structure of the ions. With a proper representation of these levels, all cross-sections and branching fractions in Equation (1) can be traced back to the many-electron transition amplitudes for the photoexcitation and ionization of atoms as calculated by the JAC toolbox mentioned above [17,18]. Indeed, the consequent use of these many-electron amplitudes in the setup of the code distinguishes JAC from most other atomic structure codes that have been described in the literature [19–21] and that might be used for photoabsorption studies.

It is the definition (1) of photoabsorption that is often applied at synchrotrons and many other light sources, regardless of further (minor, non-linear) contributions, such as the coherent formation of Fano resonances [22,23], the photo-double ionization [24] and other second-order electron and photon processes. The branching fraction $b(e \to f)$ in Equation (1) also enables one to restrict the photoabsorption cross-section to the (instantaneous) emission of single fluorescence photons or (Auger) electrons independent of any further coherent evolution of the bound-state electron density. In the present work (and implementation), we shall resort to the definition (1) but clearly distinguish between the non-resonant and resonant contributions to the photoabsorption cross-section, a user-given resolution of the spectra, to be simulated, as well as to a (normalized) distribution of initial levels that contribute to the overall photoabsorption cross-section $\sum_i w_i \, \sigma^{(absorption)} \, (\hbar \omega; i)$ with $\sum_i w_i = 1$. This simple parametrization of the photoabsorption of atoms and ions also enables us to distinguish between level- and/or subshell-resolved as well as the total photoabsorption cross-sections by just restricting the number of final levels f in the photoabsorption cross-section $\sigma^{(absorption)} \, (\hbar \omega; i) \equiv \sigma^{(absorption)} \, (\hbar \omega; i) + \sum_e \dots$ For

Atoms 2025, 13, 77 4 of 16

the treatment of the resonances $\{e\}$, moreover, the natural linewidth function $L(E_e-\hbar\omega)$, as derived quantum mechanically, is simply replaced by a Gaussian resolution function $L^{(G)}(E_e,\hbar\omega,\Gamma)$ which is solely characterized by the energy E_e and some typical width Γ , which is taken to be constant in a given region of photon frequencies. An (experimentally) constant Γ is assumed here, since the width of a resonance is determined by all its decay channels, which cannot be treated explicitly.

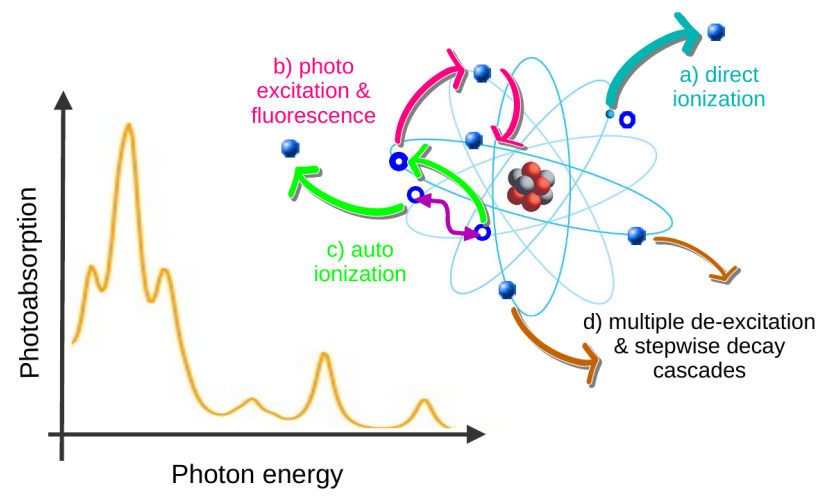


Figure 1. Overview of photoabsorption. Apart from (a) the direct photoionization of an electron into the (free-electron) continuum, it can also be excited with (b) subsequent fluorescence, (c) autoionization or (d) by following step-wise decay cascades. Dependent on the experimental setup and resolution, photoabsorption cross-sections can be distinguished for individual fine-structure levels f of the photoion, the formation of vacancies in individual shells or by taking all final levels into account that can be formed energetically due to the given photon field. See text for further discussion.

All standard computations of photoabsorption cross-sections are typically based on the electric–dipole (E1) approximation. This restriction readily truncates the set of final levels and the correlations that must be considered explicitly. While the E1 approximation can be seen dominant for all photon energies $\hbar \, \omega \, \lesssim \, 10$ keV, we can readily go in JAC also beyond this approximation by including amplitudes of higher multipoles (M1, E2, . . .) in the summation over the photoionization and/or photoexcitation channels in expression (1). Here, we shall not explain the details of these electron–photon interaction amplitudes but refer the reader to the literature instead [25]. Very little is, however, known to date regarding how these higher-multipole contributions, if at all, affect the photoabsorption cross-sections over a wider range of photon energies.

2.2. Photoabsorption Cascades

For sufficiently weak radiation fields, as seen from Equation (1), the computation of synthetic photoabsorption spectra first of all requires picking out and generating all excited and final levels, which may result from absorbing a single photon at some possible frequency within the given domain of photon energies. These final levels are formed owing to the excitation or ionization of any of the bound electrons, as far this is energetically possible, and by taking the well-known selection rules into account. Because of the quite large number of final levels, this selection of final levels requires not only an automatic and systemized procedure but also limits the amount of correlations in the quantum-mechanical setup of the final states. For the sake of simplicity, we here restrict the treatment of these levels to the absorption of a single photon, whereas the *active* electron may still come from any energetically allowed shell. Often, moreover, the emitted electron leaves a vacancy in an inner shell that is subsequently filled by autoionization or by photon emission following the quantum jump of an outer electron.

Atoms 2025, 13, 77 5 of 16

We can formalize (and simplify) the selection of final levels in the JAC toolbox by treating the photoabsorption as the sum of two independent cascade steps: photoexcitation and photoionization of an electron from any bound shell of the given atom. Since the photons can formally interact with just a single electron, only single-electron excitations of the initial—atomic or ionic—ground configuration need generally to be taken into account. This restriction neglects the (so-called) shake-up and -off contributions to the photoabsorption but keeps the treatment overall feasible as one can deal with all the generated configurations separately. Indeed, such a simplified approach closely resembles and benefits from the concept of cascade computations and simulations which have been introduced already earlier into JAC [18,26]. With these simplifications in mind, the major task is therefore to establish and implement a (new) photoabsorption cascade scheme in which the excitation and ionization transition amplitudes are treated separately from each other and are later combined only in course of the cascade simulations. Whereas such a treatment includes fewer correlations right from the very beginning, when compared to other more advanced methods [12,16], it is flexible and readily enables one to extract a number of user-selected photoabsorption cross-sections.

Analog cascade schemes have been implemented before in JAC for the stepwise decay of inner-shell holes [27,28] as well as for the radiative [29] and dielectronic recombination plasma rate coefficients [30]. In practice, any cascade model divides the prediction of the simulated spectra into (so-called) cascade computations for generating all of the underlying many-electron transition amplitudes and subsequent (cascade) simulations used to compile and extract the relevant data. In the computations, by default, the numerical evaluation of transition amplitudes is limited to a single or just a very few configurations in the configuration-interaction (CI) representation of the atomic levels involved. Different options can later be chosen for the cascade simulations to analyze the various contributions to the photoabsorption spectra. Because of the less-correlated representation of all atomic levels, such a cascade approach to photoabsorption enables one to support a wide range of shell structures of the initial ions, incident photon energies or interaction processes that may eventually lead to the absorption of photons. When compared with other methods that employ more advanced approximations to the photoabsorption, the representation of atomic bound states usually is the main difference between the known implementations if they are available at all to the public.

Any improved treatment of photoabsorption should be based of course on *well-correlated* photoexcitation and ionization amplitudes. Other, more advanced computations of photoionization cross-sections are therefore based on either the Breit–Pauli R-matrix [31] and close-coupling approximation [32] or the relativistic distorted-wave method [33]. Apart from the price of (rather) elaborate computations of all initial, inner-shell excited and final-state levels, efforts must also address the handling of the electron continua for the outgoing electrons. For most applications, in fact, such a correlated treatment of the photoabsorption cross-sections and spectra is neither feasible nor typically necessary. Apart from the sheer size of the computations, moreover, the understanding and interpretation of individual contributions can easily be lost if the representation of the intermediate resonances is based upon—the admixture of—too many configurations.

In the next section, we summarize how the photoabsorption cascade scheme is implemented into the JAC toolbox in order to estimate photoabsorption cross-sections for many ions from the periodic table as well as over a rather wide range of photon energies.

2.3. Implementation of Photoabsorption Cross-Sections Within the J_{AC} Toolbox

The JAC toolbox has been designed to compute level energies, rates and cross-sections for a wide range of atomic properties and processes [17]. Based on Dirac's relativistic

Atoms 2025, 13, 77 6 of 16

equation, this toolbox is suitable for most atoms and ions from the periodic table regardless of their detailed shell structure. Its general design makes JAC an excellent tool for modeling atomic behavior and for *quantitatively* estimating the outcome of—current and future—measurements. Apart from providing a rather general and easy-to-use toolbox for the atomic physics community, a primary design goal has been to integrate different interactions and processes within a single computational framework and, hence, to ensure good self-consistency of the generated data [34]. The basic design of JAC has been described elsewhere [17], and its code can readily be downloaded from the web [35].

Much of the recent emphasis in developing JAC has been placed upon the simulation of atomic cascades. Apart from the step-wise decay of inner-shell excited atoms and ions [36,37], we now distinguish between a number of cascade *schemes* [18] to model several advanced scenarios from atomic or plasma physics, such as electron and ion distributions [38], various kinds of plasma rate coefficients [30], or the properties of hollow ions. Here, we expand these cascade schemes in order to account for the photoabsorption of atoms and ions and to facilitate the analysis of future (merged-beam) photon-ion and photon-surface measurements or, perhaps, even the diagnostics of plasma.

Several technical cascade *approaches* have been discriminated in JAC to keep the cascade computations feasible, especially if a large number of transition amplitudes, levels and pathways arise. These approaches determine internally how accurate the level structure is modeled and, hence, which extent inter-electronic correlations are taken into account. For the photoabsorption cascade below, we use by default a single-configuration representation. However, apart from choosing the excited configurations automatically, no attempt is internally made to check that all relevant amplitudes and data are indeed computed, nor that all computed data are relevant for the subsequent simulation of the photoabsorption cross-sections.

Internally, the JAC toolbox is based entirely on Julia, a modern programming language, and greatly benefits from most of its features, such as (i) an expressive *type system;* (ii) *Just-In-Time* compilation; (iii) features for *parallelization;* or (iv) multiple dispatch that refers to the dynamic selection and execution of code [39,40]. These features have made JAC fast enough to support extensive many-electron computations.

2.4. Data Structures Useful for Photoabsorption Studies

Well-chosen data types are crucial for modern implementations (of code) independent of the given subject. Whereas the (central) role of these data types has been discussed at various places, let us briefly compile here a few of these types that are specific to the computation of photoabsorption cross-sections, which can be used to communicate the data both to and within the program.

Most central to the computation of photoabsorption cascades and spectra, perhaps, is the type Cascade.PhotoAbsorptionScheme <: Cascade.AbstractCascadeScheme. The definition of this data type is shown in the upper panel of Figure 2 along with all of its subfields that help to specify the physical parameters of the underlying model of photoabsorption. These fields require the user to select and specify the initial level or configuration of the atom or ion, the range of photon energies, the supposed excitation and ionization processes, the multipole components in the expansion of the radiation field as well as several other physical parameters. Here, we shall not discuss these subfields in much detail but simply remind the user that the internal definitions and use of all data types can be accessed at any time from JAC's documentation [35] or by using Julia's help facilities.

Atoms 2025, 13, 77 7 of 16

```
struct Cascade.PhotoAbsorptionScheme <: Cascade.AbstractCascadeScheme
  ... a struct to describe a photo-absorption calculation for an atom in some initial state/
      configuration and for a given range of photon energies, processes and multipoles, etc.
+ multipoles
                        :: Array [EmMultipole]
   .. Multipoles of the radiation field to be included into the excitation/ionization processes
+ photonEnergies
                        ::Array{Float64,1}
   .. List of photon energies (in user-selected units) for which absorption cross sections/spectra
      are to be calculated; this describes the list, distribution and resolution of energies
                         ::Array{Float64,1}
+ electronEnergies
   .. List of electron energies (in user-selected units) for which photoionization cross sections/
      spectra are to be calculated; either photonEnergies xor electronEnergies can be given.
+ excitationFromShells :: Array{Shell,1}
     List of shells from which photo-excitations are to be considered.
+ excitationToShells
                        :: Array {Shell, 1}
     List of shells into which photo-excitations are to be considered, including occupied shells.
+ initialLevelSelection ::LevelSelection
  ... Specifies the selected initial levels of some given initial-state configurations; these
      initial level numbers/symmetries always refer to the set of initial configurations
+ lValues
                         ::Array{Int64,1}
   ... Orbital angular momentum values of the free-electrons, for which partial waves are
      considered for the direct photoionization.
                                    ... True, if the direct contributions need to be calculated.
+ calcDirect
                        ::Bool
+ calcResonant
                        ::Bool
                                     ... True, if the resonant contributions need to be calculated
+ electronEnergyShift
                        ::Float64
  ... Energy shift for all bound-state energies relative to the levels from the reference
      configuration; this shift is taken in the user-defined units.
struct Cascade.PhotoAbsorptionSpectrum <: Cascade.AbstractSimulationProperty ... defines a type for
  simulating the total photo-absorption cross sections in a given interval of photon energies
  and by making use of a given set of photo-ionization and photo-excitation cross sections
+ includeIonization ::Bool
                                          ... True, if photo-ionization cross sections are calculated.
+ includeExcitation ::Bool
                                          ... True, if photo-excitation lines are to be considered.
                                          ... Widths of the resonances (user-defined units)
                      ::Float64
+ photonEnergies
                      ::Array{Float64,1}
      ... Photon energies (in user-selected units) for the simulation of photon spectra to describe the interval and resolution of the absorption cross sections.
                        :Array{Shell,1}
    ... Shells that should be included for a partial absorption cross sections; a shell is taken into
        account if its occupation is lowered in the leading configurations in the final levels of the
        photoexcitation amplitude.
+ initialOccupations :: Array{Tuple{Int64,Float64},1}
     ... List of one or several (tupels of) levels in the overall cascade tree together with their
        relative population; at least one of these tuples must be given.
                       ::Array{Configuration,1}
+ leadingConfigs
        List of leading configurations whose levels are assumed to be equally populated
        Only the initialOccupations XOR initialOccupations can be provided at a given time
```

Figure 2. Definition of the data structures Cascade.PhotoAbsorptionScheme (upper panel) and Cascade.PhotoAbsorptionSpectrum (lower panel) for the calculation of photoabsorption spectra in the Cascade module of JAC. A Cascade.PhotoAbsorptionScheme is one of the supported (cascade) schemes for performing the Cascade.Computation's; it enables the user to specify all physical and technical parameters. A PhotoAbsorptionSpectrum, in contrast, provides the information for simulating the partial or total photoabsorption cross-sections within a given interval of photon energies and by applying some preselected resolution. See text for further explanations.

The lower panel of Figure 2 displays the definition of the type Cascade. Photo AbsorptionSpectrum <: Cascade.AbstractSimulationProperty as one of the—simulated or derived—properties that are implemented in JAC. This type specifies how the data from the prior cascade computation are employed to generate the photoabsorption cross-sections within a given interval of photon energies and with a preselected resolution. In practice, this resolution is simply determined by the (list of) photonEnergies in the user-given units. For the computation of partial photoabsorption cross-sections, moreover, a list of shells should be provided to specify those shells from which contributions to the absorption cross-sections are requested. This concrete data type (property) is then given to the Cascade.Simulation and helps the user select all desired contributions to the simulated cross-section, the range of incoming photon energies, the atomic shells to be taken into account or how the levels of the initial ions were populated prior to the photoabsorption. JAC comprises in total about \sim 250 of these data structures, most of which remain however hidden to the user. A detailed description of these data types can be obtained also interactively, for instance by ? Cascade. Simulation at Julia's REPL, to recall the purpose of this struct, along with the definition of all subfields.

Atoms 2025, 13, 77 8 of 16

As outlined above, the two—computation and simulation—steps need always to be performed independently in order to obtain useful photoabsorption spectra and data. These two steps occur in the JAC toolbox in a manner quite analogous to the modeling of any other cascade scheme. In practice, however, the detailed control of these steps requires some insight from the user into the photoexcitation and absorption processes, which cannot be fully formalized in advance.

3. Photoabsorption Cross-Sections for Singly and Multiply Charged Ions

Many experimental and theoretical (atomic) photoionization studies have been reported in the literature. Despite this bulk of work and the quite detailed understanding of the electron–photon interaction in electronic-structure calculations, however, the rapid and reliable prediction of photoabsorption cross-sections and spectra have remained a challenge for atomic theory. Difficulties arise (i) from the prior but necessary assignment and generation of all resonantly excited e and final levels f in Equation (1), (ii) the insufficiently correlated representation of the ionic bound states as well as (iii) from the proper coupling and account of the electron continua, which do contribute to either the direct or the inner-shell related ionization. For medium and heavy ions, moreover, (iv) the relativistic density contraction and the fine structure of levels need to be taken into account. Below, we shall demonstrate by two examples how the photoabsorption of inner and/or valence shells can be modeled in JAC by means of the photoabsorption cascade scheme. Quite similar examples have frequently been discussed in astrophysics and at several places elsewhere [7,41].

3.1. Photoabsorption of C^+ Ions near to Their $1s \rightarrow 2p$ Resonances

In astrophysics, carbon is known as the fourth most abundant element in the solar system with a fractional abundance of about 10^{-2} relative to hydrogen. More than 100 carbon-bearing molecules have meanwhile been observed in the interstellar medium via their rotational, infrared, and/or electronic transitions [42,43]. In addition, the photoabsorption of atomic carbon in the energy region below and near the $1s^{-1}$ threshold has been observed by Chandra and XMM-Newton in a variety of X-ray binary spectra and have enabled one to draw conclusions about the level composition and, hence, the temperature of selected astrophysical objects [44,45]. In particular, the photoabsorption of C^+ ions in their low-lying $1s^2 2s^2 2p^{-2}P$ ground and $1s^2 2s 2p^{2-4}P$ metastable terms have attracted recent spectroscopic interest [46]. For photon energies $285 \le \hbar \omega \le 326$ eV, i.e., near to and above the K-shell single-ionization threshold, Müller and coworkers [46] studied the single, double and triple ionization of the C^+ ion by photon irradiation at a synchrotron in quite unprecedented detail.

In JAC, we can readily estimate the photoabsorption cross-sections of C^+ ions in their $1s^2\,2s^2\,2p$ ground configuration by following the script in Figure 3 for performing cascade computations (upper panel) and simulations (lower panel). In these calculations, a Cascade .PhotoAbsorptionScheme has been specified for the three photon energies $\hbar\,\omega = 285$, 290, 295 eV to estimate the direct contribution to the photoaborption cross-section for the excitation (ionization) of an electron from the 1s and 2s shells (fromShells) into either the 2p or 3p shells (toShells) or directly into the continuum. From these shell lists, all possible (five-electron) configurations are then generated automatically, and their mean excitation energy is compared to the incoming photon energies. Within the given interval $285 \le \hbar\,\omega \le 295$ eV of incoming photon energies, furthermore, the selected photoexcitations are taken into account at their calculated resonance position. In the input of Figure 3, the incorporation of the direct and resonant parts to the total photoabsorption cross-sections is readily determined by the two logical flags calcDirect and calcResonant,

Atoms 2025, 13, 77 9 of 16

respectively. Obviously, only those photoexcitation and ionization data are later available for the simulation of cross-sections, which have been generated (computed) before. This is in contrast to the subsequent simulations, in which parts of the generated data can be still omitted from the simulated spectra by using some proper input script.

Apart from the photoabsorption scheme, the radial grid must be specified initially in the cascade computations, which is a choice that will affect all subsequent electronic-structure calculations. Photoabsorption data are generated automatically for all levels from the initial configuration(s). In the subsequent simulations (the lower panel of Figure 3), we then need to provide the amplitude data from the first step, the photon energies (of the usually much finer energy mesh) as well as the user-specified selection of the different contributions. Here, we can also restrict the interval of photon energies and the population of the initial fine-structure levels by providing their relative weights. Moreover, we may overwrite the shells of the initial ions that *do* contribute to the photoabsorption, whereas all occupied shells are taken into account if an empty shell list (Shell[] as default) is provided in these simulations. Further technical parameters can be utilized (or could readily be added to the code) to make such photoabsorption calculations feasible for an even wider range of applications and for other useful restrictions.

```
\# Photoabsorption of C^+ near to the 1s -> 2p resonances: Computation
calcDirect = true
calcResonant = true
fromShells = [Shell("1s"), Shell("2s")]
            = [Shell("2p"), Shell("3p")]
toShells
grid
     = Radial.Grid(Radial.Grid(false), rnt=4.0e-6, h=5.0e-2, hp=0.6e-2, rbox=10.0)
      = "Photoabsorption of C^+: Computation"
pScheme = Cascade.PhotoAbsorptionScheme([E1], [en for en = 285.0 :5.0 :295.0], Float64[],
                              fromShells, toShells, calcDirect, calcResonant, 0., 0.)
comp
       = Cascade.Computation(Cascade.Computation(); nuclearModel = Nuclear.Model(6.),
                              grid = grid, name = name, scheme = pScheme,
                              approach = Cascade.AverageSCA(),
                              initialConfigs = [Configuration("1s^2 2s^2 2p")] )
wb = perform(comp)
```

Figure 3. Input to the JAC toolbox for the cascade computation (**upper panel**) and simulation (**lower panel**) of the photoabsorption spectra of C^+ ions, being initially in their $1s^22s^22p$ ground configuration. In the upper computations, the incident light is considered at the three discrete photon energies $\hbar\,\omega=285$, 290, 295 eV in order to estimate the direct photoionization contribution to the photoabsorption within the electric-dipole (E1) approximation, whereas all 1s, $2s\to 2p$, 3p excitations (fromShells \to toShells) are considered at their calculated resonance position in the interval $285 \le \hbar\,\omega \le 295$ eV. The simulations, in contrast, assume a much finer energy grid of $\Delta\,E=0.2\,\mathrm{eV}$ to make both the direct and resonant contributions to the photoabsorption visible. The photoexcitation and ionization amplitudes are first stored in the file cascade-photoabsorption-computations. jld and later processed within the subsequent simulations. See text for further discussions.

Figure 4 displays the photoabsorption cross-section as function of the incident photon energy in the energy range $286 \le \hbar \omega \le 292$ eV for C⁺ ions in their initial $1s^2 2s^2 2p$ ground configuration. The left panel of this figure shows the simulated cross-sections

Atoms 2025, 13, 77 10 of 16

for the two initial $^2P_{1/2,3/2}$ fine-structure levels as obtained from the present (cascade) computations and simulations. On the right panel, the total photoabsorption cross-section is shown as measured at the PIPE facility in Hamburg [46]. In these measurements, it was supposed that about 90% of the ions are in the $2s^2P^2$ ground-term and the remaining 10% are in the $2s^2P^2$ metastable term. The simulated photoabsorption cross-section for such an admixture of ground and meta-stable levels is shown as the red curve in the left panel of Figure 4. Overall, a reasonable agreement is found between the measured and simulated spectra despite all the visible differences. The calculated fine structure of the $1s^2 2s^2 2p$ ground levels appears slightly larger than in the measurements owing to the approximate representation. The single-configuration approach in the underlying cascade computation here limits a more detailed comparison of individual resonances. No further attempts have been undertaken to improve the position and intensities of individual lines. In most photoabsorption spectra and for the excitation and ionization of subvalence electrons, the fine structure can typically be neglected, at least, as long as the level splitting is (much) smaller than the total width of the resonances.

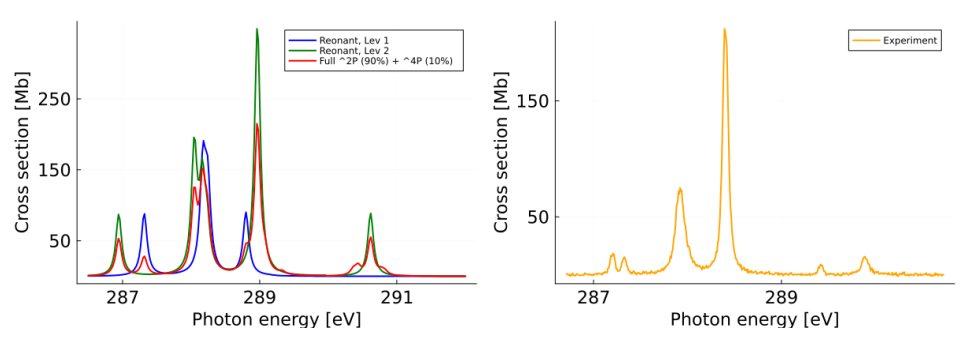


Figure 4. Photoabsorption cross-section as the function of the incident photon energy in the energy range $286 \le \hbar \omega \le 292$ eV for C⁺ ions in their initial $1s^2 2s^2 2p$ ground configuration. (**Left panel**) Comparison of the simulated photoabsorption spectra for the population of the two $^2P_{1/2}$ (Lev 1, blue solid line), $^2P_{3/2}$ (Lev 2, green solid line) ground levels as well as for an initial admixture of the 2P (90%) and the metastable 4P (10%) terms (red solid line). Both the direct and resonant contributions are taken into account in this figure. (**Right panel**) Total photoabsorption cross-sections [data are extracted from Figure 4 of Ref. [46]] measured at the PIPE facility in Hamburg (orange solid line). In these experiments, it was supposed as well by Müller and coworkers that about 90% of the ions are in the $2s^2 2p^2$ P ground and 10% are in the $2s^2 2p^2$ 4P metastable term.

3.2. Photoabsorption of Xe²⁺ Ions Due to Excitations from Different Valence Shells

The photoabsorption of xenon in the 10–200 eV energy range has been frequently analyzed in atomic and molecular physics for its application in vacuum ultraviolet (VUV) spectroscopy as well as in astro and plasma physics. At synchrotron light sources, for instance, xenon's well-explored absorption spectrum has been utilized to calibrate monochromators and detectors. In particular, the strong 4d giant resonance has often been explored to test and validate (benchmark) quantum many-body theories, such as the random-phase approximation without and with exchange [47,48]. While several outer-shell (valence) excitations primarily occur due to $5p \rightarrow ns/nd$ Rydberg series in the 10–20 eV region, a set of autoionizing resonances and inner-shell excitation due to $4d \rightarrow \varepsilon \ell$ photoexcitations dominate the photoabsorption for 20–120 eV. The strong $4d^{-1}$ shape resonance (giant resonance) has a broad peak and is today a known hallmark of xenon [49–51]. This spectral feature has sometimes been interpreted as a collective excitation of the 4d electrons by using arguments from the classical electron gas. In contrast to this behavior, however, most other discrete absorption lines due to different bound–bound transitions remain sharp and well defined in high-resolution spectra.

Atoms 2025, 13, 77

Xenon has been applied also in spacecraft ion thrusters and propulsion systems. As a noble gas, it does chemically not react with other thruster components and, hence, may simplify material selection and maintenance [52,53]. Moreover, neutral xenon atoms are rather heavy and have a relatively low ionization energy of 12.13 eV, which reduces the electrical power needed to operate the ion thrusters. A similar interest arises from the emission spectra of planetary exospheres or comet tails as well as in high-temperature plasma devices, such as tokamaks or Z-pinches, where xenon has been applied to study radiative energy losses via inner-shell excitations. For all these applications, it has been found essential to better understand the behavior and radiation characteristics of xenon ions in multiple and high charge states.

From the viewpoint of atomic theory, xenon ions (Xe, Z=54) still have a reasonably simple shell structure. The low charge states of xenon Xe^{q+}, $q=1,\ldots,5$ all exhibit an open 5p valence shell along with the closed $4d^{10}\,5s^2$ subvalence core. For a wide range of extreme ultraviolet (XUV) photon energies, the absorption spectra of Xe^{q+} ions therefore show a great number of (unresolved) resonances, the so-called unresolved transition array (UTA), that can hardly be classified separately [54,55]. For the Xe⁺ and Xe⁺ ions, for example, Anderson and coworkers [56] measured partial and total absolute cross-sections for the photoionization at selected photon energy intervals and compared them with calculated data as obtained by the random phase approximation.

As a second example, we shall therefore compute the photoabsorption, respectively the photoionization, of Xe^{2+} ions in the $5p^4$ 3P_2 ground level over the photon energy range 10–200 eV. Apart from the direct photoionization of the 4d+5s+5p (sub-)valence electrons, the photoabsorption spectrum is mainly determined by overlapping resonances due to the excitation of these electrons at characteristic positions in the spectrum. For these reasons, emphasis needs to be placed on both the photoexcitation and ionization of electrons. Here, we shall not discuss the (Julia) input to this example, which follows similar lines as above, but instead will demonstrate how different assumptions can be readily made and compared with each other in calculating the photoabsorption cross-sections with regard to the (inner) shell contributions.

Indeed, our cascade approach to the photoabsorption of atoms and ions enables us to selectively analyze contributions from the photoexcitation and ionization for (i) individual electron shells (fromShells, toShells), (ii) the partial-wave character of the outgoing electrons or (iii) for the superposition of different initial levels. For further details about the corresponding input, we refer the reader to the documentation of JAC and its help facilities. In the figures below, we make use of these (selected) features to distinguish different contributions to the overall photoabsorption, for instance, by displaying shell-resolved cross-sections, in which the occupation of selected shells is lowered by '1' if analyzed with regard to its leading configuration of the initial and final levels. Explicitly, the left panel of Figure 5 compares the partial photoionization cross-section from the 5s + 5p valence electrons (blue line) with those from the 4d (green line) and the 4s + 4p core electrons (cyan line). In the right panel of Figure 5, we compare instead the partial 4d (blue lines) and total photoionization cross-section (red lines) by including the contributions of all shells as obtained in (solid lines) and velocity gauge (dashed lines). Resonant contributions to the photoabsorption are not included in this figure. The restricted wave function expansion in our cascade approach still prevents a closer agreement between the two gauges. Naturally, other classes of inner- and valence-shell excitations could be analyzed in a similar way.

Figure 6 compares the total photoabsorption spectrum of Xe²⁺ ions in the photon energy region 10–200 eV. The total cross-section from measurements (orange line) are compared with computations in which the direct and resonant contributions were simply

Atoms 2025, 13, 77

added in velocity (pink dashed line; +30 Mb) and length gauge (red solid line; +60 Mb), respectively. For the sake of visibility, the synthesized spectra are each shifted by +30 Mb.

Of course, similar computations can also be performed also for other charge states and/or elements. While the present implementation supports straightforward access to the photoabsorption spectra (in different approximations), it usually provides a reasonable though still incomplete agreement with available measurements and will *not* overcome all the challenges associated with inner-shell phenomena. For heavy ions with a complex and often open-shell structure, the deviations between the simulations and experiment can usually be attributed to (a) their shell structure with nearly degenerate *d*- and *f*-shells, (b) the approximate representation of the photoexcited and ionized levels in expression (1), (c) the simplified treatment of the electron continuum as distorted waves as well as (d) to the single-configuration approach in the underlying cascade model with all the "missing" correlations. However, these limitations indicate once more the challenge and intricacy in predicting useful photoabsorption spectra over a large range of photon energies. In practice, the applied cascade scheme clearly helps to reduce previous difficulties in generating a sufficiently large number of final states and in dealing with good ranges of (incoming) photon energies.

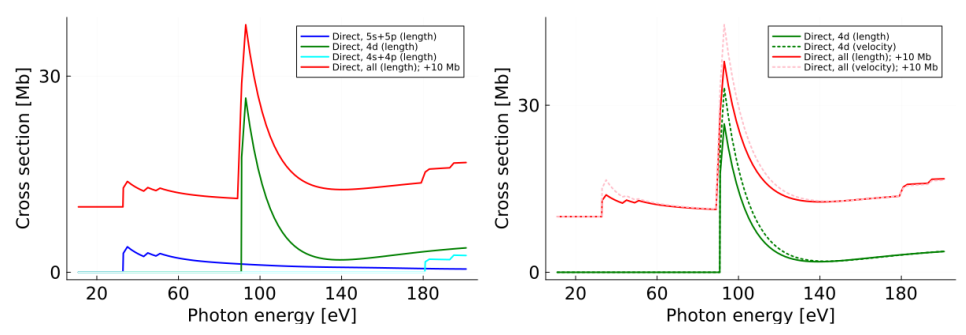


Figure 5. Selected contributions to the photoionization of Xe^{2+} ions in their $5p^4$ 3P_2 ground level in the energy region 10–200 eV. (**Left panel**) The partial photoionization cross-section from the 5s+5p valence electrons (blue solid line) is compared with those from the 4d (green solid line) and 4s+4p core electrons (cyan solid line). The total photoabsorption cross-section (red solid line) comprises the sum of all three contributions. All results are shown in the length gauge in this left panel. (**Right panel**) Partial 4d (green lines) and total photoionization cross-section (red lines) for the ionization of an electron from the 4s+4p+4d+5s+5p shells in length (solid lines) and velocity gauge (dashed lines). No resonant contributions to the photoabsorption are yet included in this figure. For the sake of visibility, all the total cross-sections are shifted by +10 Mb.

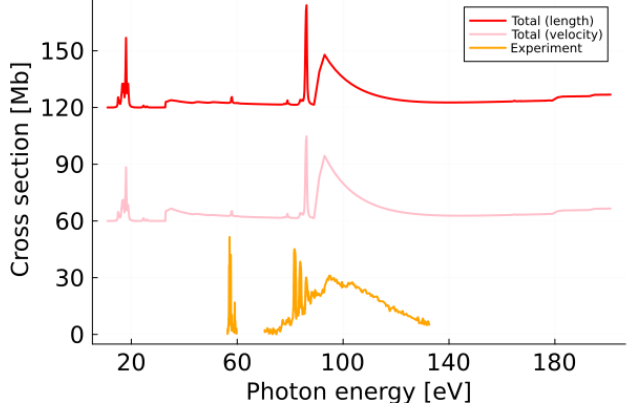


Figure 6. Total photoabsorption spectrum of Xe^{2+} ions in the photon energy region 10–200 eV. Total cross-section from measurements (orange line) are compared with computations by adding the direct and resonant contributions in velocity (pink dashed line; +30 Mb) and length gauge (red solid line; +60 Mb), which are each shifted by +30 Mb for the sake of visibility.

Atoms 2025, 13, 77

4. Summary and Conclusions

For several decades, the photoabsorption of atoms and ions has been a key tool to better understand light–matter interactions in many research areas. Apart from quick estimates of selected features in the absorption spectra, detailed computations of (photoabsorption) cross-sections over a wide range of photon energies are required in order to model the behavior of matter under different circumstances with applications in nuclear fusion, X-ray generation, and other fields. Here, we have implemented and discussed a relativistic cascade model within the JAC toolbox for estimating the photoabsorption of several, if not most, atoms and ions with complex shell structures across the periodic table. This model helps (i) distinguish between level- and shell-resolved as well as total photoabsorption cross-sections (ii) by assuming a predefined initial level population of the ions. It also supports (iii) the account of the (relativistic) fine-structure splitting, (iv) fast access as well as (v) the choice of user-defined units in evaluating the cross-sections.

Examples are shown especially for the photoabsorption of C^+ ions near their 1s-2p excitation threshold and for Xe^{2+} ions in the photon energy range 10–200 eV. The input script for C^+ ions illustrates how easily these calculations can be performed by the current implementation. While the accuracy and resolution of the predicted photoabsortion spectra remain limited in such a cascade model, mainly because of the additive treatment of resonances and the neglect of certain correlations, the present implementation is suitable for most ions and, hence, allows surveys of resonances along different isoelectronic sequences. Further advancements of this cascade approach to photoabsorption might refer in the future to a faster diagonalization of the (large number of) Hamiltonian matrices and a more efficient treatment of the continuum orbitals.

Modern photon-ion spectroscopy has revealed many additional features beyond those associated with the—direct or resonant — ionization of individual electrons from neutral atoms. For example, the photon-ion merged-beams method [57] helps compensate for a low target density by providing an elongated interaction region of about 1 m length where the photon and the ion beams move coaxially. Such merged-beam experiments with ions at synchrotrons allow, for example, to resolve photo-double ionization and various shake-up and shake-off processes to the photoabsorption of ions even if these contributions can often be neglected in the total absorption spectra [58]. For these processes as well, the JAC toolbox provides a powerful framework to analyze ongoing experiments.

Author Contributions: Methodology, S.F. and S.S.; software, S.F. and A.K.S.; writing—review and editing, S.F., L.S. and S.S. All authors have read and agreed to the published version of the manuscript.

Funding: This research has been funded in part by the German Federal Ministry for Research, Technology and Space (BMFTR) within the ErUM-Pro funding scheme under contracts 05P24RG2 and 05P24SJA.

Acknowledgments: During the preparation of this manuscript, the authors used GPT-5 for the purposes of English improvement. The authors have reviewed and edited the output and take full responsibility for the content of this publication.

Conflicts of Interest: The author declares no conflicts of interest.

References

- 1. Brandt, W.; Eder, L.; Lundqvist, S. Atomic photoabsorption cross sections. *J. Quant. Spectrosc. Radiat. Transf.* **1967**, *1*, 185. [CrossRef]
- 2. Olney, T.N.; Cann, N.M.; Cooper, G.; Brion, C.E. Absolute scale determination for photoabsorption spectra and the calculation of molecular properties using dipole sum-rules. *Chem. Phys.* **1997**, 223, 59. [CrossRef]
- 3. Norrish, R.G.W.; Porter, G. Chemical reactions produced by very high light intensities. Nature 1949, 164, 4172. [CrossRef]

Atoms 2025, 13, 77 14 of 16

4. Shikawa, K.; Felderhof, B.U.; Blenski, T.; Cichocki, B. Photoabsorption by an ion immersed in a plasma at any temperature. *J. Plasma Phys.* **1998**, *60*, 787. [CrossRef]

- 5. Salzmann, D.; Wendin, G. Calculation of the photoabsorption coefficient in a hot and dense aluminum plasma. *Phys. Rev. A* **1978**, 18, 2695. [CrossRef]
- 6. Bhatia, A.K. Scattering and its applications to various atomic processes: Elastic scattering, resonances, photoabsorption, Rydberg states, and opacity of the atmosphere of the Sun and stellar objects. *Atoms* **2020**, *8*, 78. [CrossRef]
- 7. Shulyak, D.; Tsymbal, V.; Ryabchikova, T.; Stütz, C.; Weiss, W.W. Line-by-line opacity stellar model atmospheres. *Astron. Astrophys.* **2004**, *428*, 993. [CrossRef]
- 8. Hisaka, A.; Sasakura, Y. Light scattering characteristics of biological tissues in coaxial ultrasound-modulated optical tomography. *Jap. J. Appl. Phys.* **2009**, *48*, 067002. [CrossRef]
- 9. Nakayama, M.; Masai, K. Properties of photoionized gas in accretion-powered sources. *Astron. Astrophys.* **2001**, *375*, 328. [CrossRef]
- 10. Gorti, U.; Hollenbach, D. Models of chemistry, thermal balance, and infrared spectra from intermediate-aged disks around G and K stars. *Astrophys. J.* **2004**, *613*, 424. [CrossRef]
- 11. Matsuzawa, N.N.; Ishitani, A.; Dixon, D.A.; Uda, T. Time-dependent density functional theory calculations of photoabsorption spectra in the vacuum ultraviolet region. *J. Phys. Chem. A* **2001**, *105*, 4953. [CrossRef]
- 12. Tenorio, B.N.C.; Nascimento, M.A.C.; Rocha, A.B. Time-dependent density functional theory description of total photoabsorption cross sections. *J. Chem. Phys.* **2018**, *148*, 074104. [CrossRef]
- 13. Senashenko, V.S.; Wague, A. Resonance photoabsorption of the helium atom in the vicinity of the (3*s*3*p*) ¹*P* resonance. *J. Phys. B* **1979**, 12, L269. [CrossRef]
- 14. Perry-Sassmannshausen, A.; Buhr, T.; Borovik, A., Jr.; Martins, M.; Reinwardt, S.; Ricz, S.; Stock, S.O.; Trinter, F.; Müller, A.; Fritzsche, S.; et al. Multiple photodetachment of carbon anions via single and double core-hole creation. *Phys. Rev. Lett.* **2020**, 124, 083203. [CrossRef] [PubMed]
- 15. Wu, Z.W.; Wang, J.Q.; Li, Y.; An, Y.H.; Fritzsche, S. Relativistic R-matrix calculations for the photoionization of W⁶¹⁺ ions. *Phys. Plasma* **2024**, *31*, 043301. [CrossRef]
- 16. Stetina, T.F.; Sun, S.; Williams-Young, D.B.; Li, X. Modeling magneto-photoabsorption using time-dependent complex generalized Hartree-Fock. *Chem. Photo Chem.* **2019**, *3*, 739. [CrossRef]
- 17. Fritzsche, S. A fresh computational approach to atomic structures, processes and cascades. *Comp. Phys. Commun.* **2019**, 240, 1–14. [CrossRef]
- 18. Fritzsche, S.; Sahoo, A.K.; Sharma, L.; Wu, Z.W.; Schippers, S. Merits of atomic cascade computations. *Eur. Phys. J. D* **2024**, *78*, 75. [CrossRef]
- 19. Kramida, A. Cowan code: 50 years of growing impact on atomic physics. Atoms 2019, 7, 64. [CrossRef]
- 20. Gu, L.; Raassen, A.J.J.; Mao, J.; de Plaa, J.; Shah, C.; Pinto, C.; Werner, N.; Simionescu, A.; Mernier, F.; Kaastra, J.S. X-ray spectra of the Fe-L complex. *Astron. Astrophys.* **2019**, *627*, A51. [CrossRef]
- 21. Fritzsche, S. The RATIP program for relativistic calculations of atomic transition, ionization and recombination properties. *Comp. Phys. Commun.* **2012**, *183*, 1525. [CrossRef]
- 22. Ihra, W. Statistical theory of Fano resonances in atomic and molecular photoabsorption. Phys. Rev. A 2002, 66, 020701. [CrossRef]
- 23. Rothhardt, J.; Hädrich, S.; Demmler, S.; Krebs, M.; Fritzsche, S.; Limpert, J.; Tünnermann, A. Enhancing the macroscopic yield of narrow-band high-order harmonic generation by Fano resonances. *Phys. Rev. Lett.* **2014**, *112*, 233002. [CrossRef]
- 24. Rouvellou, B.; Journel, L.; Bizau, J.M.; Cubaynes, D.; Wuilleumier, F.J.; Richter, M.; Selbmann, K.-H.; Zimmermann, P. Direct double photoionization of atomic sodium. *Phys. Rev. A* **1994**, *50*, 4868. [CrossRef] [PubMed]
- 25. Starace, A.F. Photoionization of atoms. In *Springer Handbook of Atomic, Molecular, and Optical Physics*; Springer Science & Business Media: Berlin/Heidelberg, Germany, 2006; p. 283.
- 26. Fritzsche, S.; Palmeri, P.; Schippers, S. Atomic cascade computations. Symmetry 2021, 13, 520. [CrossRef]
- 27. Schippers, S.; Borovik, A., Jr.; Buhr, T.; Hellhund, J.; Holste, K.; Kilcoyne, A.L.D.; Klumpp, S.; Martins, M.; Müller, A.; Ricz, S.; et al. Stepwise contraction of the *nf* Rydberg shells in the 3*d* photoionization of multiply-charged xenon ions. *J. Phys. B* **2015**, 48, 144003. [CrossRef]
- 28. Beerwerth, R.; Buhr, T.; Perry-Sassmannshausen, A.; Stock, S.O.; Bari, S.; Holste, K.; Kilcoyne, A.L.D.; Reinwardt, S.; Ricz, S.; Savin, D.W.; et al. Near L-edge single and multiple photoionization of triply charged iron ions. *Astrophys. J.* 2019, 887, 189. [CrossRef]
- 29. Fritzsche, S.; Maiorova, A.V.; Wu, Z.W. Radiative recombination plasma rate coefficients for multiply charged ions. *Atoms* **2023**, *11*, 50. [CrossRef]
- Fritzsche, S. Dielectronic recombination strengths and plasma rate coefficients of multiply charged ions. Astron. Astrophys. 2021, 656, A163. [CrossRef]

Atoms 2025, 13, 77 15 of 16

31. Donnelly, D.; Bell, K.L.; Hibbert, A. Breit-Pauli R-matrix calculation of the 3*p* photoabsorption of singly ionized chromium. *J. Phys. B* **1997**, *30*, L285. [CrossRef]

- 32. Garcia, J.; Mendoza, C.; Bautista, M.A.; Gorczyca, T.W.; Kallman, T.R.; Palmeri, P. K-shell photoabsorption of oxygen ions. *Astrophys. J. Suppl. Ser.* **2005**, *158*, 68. [CrossRef]
- 33. Delahaye, F.; Ballance, C.P.; Smyth, R.T.; Badnell, N.R. Quantitative comparison of opacities calculated using the R-matrix and distorted-wave methods: Fe XVII. *Mon. Not. R. Astron. Soc.* **2021**, *508*, 421. [CrossRef]
- 34. Fritzsche, S. Application of symmetry-adapted atomic amplitudes. Atoms 2022, 10, 127. [CrossRef]
- 35. Fritzsche, S. JAC: User Guide, Compendium & Theoretical Background. Available online: https://github.com/OpenJAC/JAC.jl (accessed on 10 July 2025).
- 36. Schippers, S.; Beerwerth, R.; Abrok, L.; Bari, S.; Buhr, T.; Martins, M.; Ricz, S.; Viefhaus, J.; Fritzsche, S.; Müller, A. Prominent role of multielectron processes in K-shell double and triple photodetachment of oxygen anions. *Phys. Rev. A* **2016**, *94*, 041401. [CrossRef]
- 37. Müller, A.; Müller, A.; Martins, M.; Borovik, A., Jr.; Buhr, T.; Perry-Sassmannshausen, A.; Reinwardt, S.; Trinter, F.; Schippers, S.; Fritzsche, S.; et al. Role of L-shell single and double core-hole production and decay in m-fold $(1 \le m \le 6)$ photoionization of the Ar⁺ ion. *Phys. Rev. A* **2021**, *104*, 033105. [CrossRef]
- 38. Schippers, S.; Martins, M.; Beerwerth, R.; Bari, S.; Holste, K.; Schubert, K.; Viefhaus, J.; Savin, D.W.; Fritzsche, S.; Müller, A. Near L-edge single and multiple photoionization of singly charged iron ions. *Astrophys. J.* **2017**, *849*, 5. [CrossRef]
- 39. Julia 1.10 Documentation. Available online: https://docs.julialang.org/ (accessed on 5 May 2025).
- 40. Bezanson, J.; Chen, J.; Chung, B.; Karpinski, S.; Shah, V.B.; Vitek, J.; Zoubritzky, J. Julia: Dynamism and performance reconciled by design. In *Proceedings of the ACM on Programming Languages*; Association for Computing Machinery: New York, NY, USA, 2018; Volume 2, p. 120.
- 41. Heays, A.N.; Bosman, A.V.; Van Dishoeck, E.F. Photodissociation and photoionisation of atoms and molecules of astrophysical interest. *Astron. Astrophys.* **2017**, *602*, A105. [CrossRef]
- 42. Ehrenfreund, P.; Sephton, M.A. Carbon molecules in space: From astrochemistry to astrobiology. *Faraday Discuss.* **2006**, 133, 277. [CrossRef]
- 43. Ziurys, L.M.; Halfen, D.T.; Geppert, W.; Aikawa, Y. Following the interstellar history of carbon: From the interiors of stars to the surfaces of planets. *Astrobiology* **2016**, *16*, 997. [CrossRef]
- 44. Weisskopf, M.C.; Aldcroft, T.L.; Bautz, M.; Cameron, R.A.; Dewey, D.; Drake, J.J.; Grant, C.E.; Marshall, H.L.; Murray, S.S. An overview of the performance of the Chandra x-ray observatory. *Exp. Astron.* **2003**, *16*, 1–68. [CrossRef]
- 45. Psaradaki, I.; Corrales, L.; Werk, J.; Jensen, A.G.; Costantini, E.; Mehdipour, M.; Cilley, R.; Schulz, N.; Kaastra, J.; García, J.A.; et al. Elemental abundances in the diffuse interstellar medium from joint far-ultraviolet and x-ray spectroscopy: Iron, oxygen, carbon, and sulfur. *Astron. J.* 2024, 167, 217. [CrossRef]
- 46. Müller, A.; Müller, A.; Borovik, A., Jr.; Buhr, T.; Hellhund, J.; Holste, K.; Kilcoyne, A.L.D.; Klumpp, S.; Martins, M.; Ricz, S. Near-K-edge single, double, and triple photoionization of C⁺ ions. *Phys. Rev. A* **2018**, *97*, 013409. [CrossRef]
- 47. Parpia, F.A.; Johnson, W.R.; Radojevic, V. Application of the relativistic local-density approximation to photoionization of the outer shells of neon, argon, krypton, and xenon. *Phys. Rev. A* **1984**, 29, 3173. [CrossRef]
- 48. Kutzner, M.M.; Radojevic, V.; Kelly, H.P. Extended photoionization calculations for xenon. Phys. Rev. A 1989, 40, 5052. [CrossRef]
- 49. Connerade, J.P.; Lane, A.M. Interacting resonances in atomic spectroscopy. Rep. Prog. Phys. 1988, 51, 1439. [CrossRef]
- 50. Henke, B.L.; Gullikson, E.M.; Davis, J.C. X-ray interactions: Photoabsorption, scattering, transmission, and reflection at E = 50–30.000 eV, Z = 1–92. *At. Data Nucl. Data Tables* **1993**, *54*, 181. [CrossRef]
- 51. Magrakvelidze, M.; Madjet, M.E.A.; Chakraborty, H.S. Attosecond delay of xenon 4*d* photoionization at the giant resonance and Cooper minimum. *Phys. Rev. A* **2016**, *94*, 013429. [CrossRef]
- 52. Holste, K.; Dietz, P.; Scharmann, S.; Keil, K.; Henning, T.; Zschätzsch, D.; Reitemeyer, M.; Nauschütt, B.; Kiefer, F.; Kunze, F.; et al. Ion thrusters for electric propulsion: Scientific issues developing a niche technology into a game changer. *Rev. Sci. Instr.* 2020, 91, 6. [CrossRef] [PubMed]
- 53. Eichhorn, C.; Löhle, S.; Fasoulas, S.; Leiter, H.; Fritzsche, S.; Auweter–Kurtz, M. Photon laser-induced fluorescence of neutral xenon in a thin xenon plasma. *J. Propuls. Power* **2012**, *28*, 1116. [CrossRef]
- 54. Fahy, K.; Dunne, P.; McKinney, L.; O'Sullivan, G.; Sokell, E.; White, J.; Aguilar, A.; Pomeroy, J.M.; Tan, J.N.; Blagojević, B.; et al. UTA versus line emission for EUVL: Studies on xenon emission at the NIST EBIT. *J. Phys. D* **2004**, *37*, 3225. [CrossRef]
- 55. Mazevet, S.; Abdallah, J. Mixed UTA and detailed line treatment for mid-Z opacity and spectral calculations. *J. Phys. B* **2006**, 39, 3419. [CrossRef]
- 56. Andersen, P.; Andersen, T.; Folkmann, F.; Ivanov, V.K.; Kjeldsen, H.; West, J.B. Absolute crosssections for the photoionization of 4d electrons in Xe⁺ and Xe²⁺ ions. *J. Phys. B* **2001**, *34*, 2009. [CrossRef]

Atoms 2025, 13, 77 16 of 16

57. Schippers, S.; Buhr, T.; Borovik, A., Jr.; Holste, K.; Perry-Sassmannshausen, A.; Mertens, K.; Reinwardt, S.; Martins, M.; Klumpp, S.; Schubert, K.; et al. The photon-ion merged-beams experiment PIPE at PETRA III—The first five years. *X-Ray Spectrosc.* **2020**, 49, 11. [CrossRef]

58. Schippers, S.; Perry-Sassmannshausen, A.; Buhr, T.; Martins, M.; Fritzsche, S.; Müller, A. Multiple photodetachment of atomic anions via single and double core-hole creation. *J. Phys. B* **2020**, *53*, 192001. [CrossRef]

Disclaimer/Publisher's Note: The statements, opinions and data contained in all publications are solely those of the individual author(s) and contributor(s) and not of MDPI and/or the editor(s). MDPI and/or the editor(s) disclaim responsibility for any injury to people or property resulting from any ideas, methods, instructions or products referred to in the content.